Soft magnetic lithography and giant magnetoresistance in superconducting/ferromagnetic hybrids

V. K. Vlasko-Vlasov, U. Welp, A. Imre,* D. Rosenmann, J. Pearson, and W. K. Kwok
Materials Science Division, Argonne National Laboratory, Argonne, Illinois 60439, USA
(Received 1 October 2008; published 18 December 2008)

We demonstrate an approach to create a tunable pinning potential in a superconducting/ferromagnetic (SC/FM) hybrid, allowing the switching of their electronic properties through the application of a small magnetic field. Using direct magneto-optical imaging, macroscopic transport, and magnetic measurements, we show that the alignment of stripe domains in the ferromagnet provides a remarkable directionality for the superconducting vortex motion. An analysis of the anisotropic flux motion demonstrates a substantial critical current anisotropy in the superconductor. The possibility of aligning stable lattices of stripe domains in select directions using in-plane magnetic fields allows the realization of soft magnetic lithography for efficient manipulation of supercurrent flow in SC/FM bilayers. Furthermore, in our samples we observed a pronounced magnetoresistance effect yielding 4 orders of magnitude resistivity change in a few millitesla in-plane field.

DOI: 10.1103/PhysRevB.78.214511 PACS number(s): 74.81.Bd, 74.70.−b, 74.25.−q

I. INTRODUCTION

The fundamental incompatibility of superconductivity (SC) and ferromagnetism (FM) caused by their mutually exclusive spin alignment requirements typically results in the *deterioration* of the SC properties when films of SC and FM materials are brought into close contact.[1–6] Both the *short-range* proximity effects caused by the FM exchange, which tends to align antiparallel spins of electrons in the SC Cooper pairs, and the *long-range* orbital effects, depairing electrons due to stray fields of FM domains, suppress the superconductivity. There is a wide variety of intriguing physical phenomena which emerge from these effects in superconducting/ferromagnetic (SC/FM) hybrids, ranging from variable phase Josephson coupling[7] and tunable SC transition temperature[8–11] to field induced or reentrant superconductivity and the appearance of SC channels along FM domain walls.[12–17] These phenomena were extensively studied both theoretically and experimentally and have been thoroughly discussed in recent reviews.[18–21]

In contrast, there is a set of phenomena that facilitate the *improvement* of SC properties, driven by the interactions of the SC vortices with the stray fields and magnetization of the FM layer (see review[20]). These phenomena can promote strong *magnetic pinning* effect in SC/FM hybrids, resulting in the enhancement of the superconducting critical current.[22–29] Typically the magnetic pinning of vortices is achieved using lithographically defined arrays of magnetic dots of different shapes and anisotropies. These magnetic structures produce local stray fields which attract or repel vortices depending on their mutual polarity.[26,29] Such arrays form spatially *fixed* periodic potential, leading to resonantly increased SC currents at *matching* magnetic fields when an integer number of vortices occupies the array period although their action can be somewhat altered by remagnetizing the magnetic dots.[28–31] Here we demonstrate an approach to engineer an *in situ tunable anisotropic* pinning potential using fine-scale stripe domains that can be oriented along any chosen direction in the plane of the SC/FM bilayer. Such an oriented array of stripes provides a sturdy pathway for directional vortex motion in the SC layer along the FM domain walls and induces a strong anisotropy in the superconducting critical currents. This was directly observed in our recent experiments on $NbSe_2$ single crystals covered with a Permalloy (Py) film.[32] Here we show that the anisotropy of vortex motion becomes much more distinct in SC films contacting a magnetic layer. In our samples, the anisotropy of the transport current noticeably increases near the SC transition when other pinning mechanisms weaken. We demonstrate that the preferential current axis can be easily tuned in a chosen direction by the rotation of the magnetic stripe domains allowing the realization of a superconducting current switch or current redistributor, which can steer current in any select direction in the film plane. For applied current oriented perpendicular to the domain walls, we found an unusually large magnetoresistance where the resistivity changed by 4 orders of magnitude in an in-plane field of a few millitesla. This effect is much larger than any reported magnetoresistance value[33–35] and its possible origin could be the granularity of our films.

II. EXPERIMENT

We studied bilayers of 0.7 μm ferromagnetic Py (Fe81Ni19) films covered with a 1 μm superconducting lead (Pb) coating. First, the Py films were magnetron sputtered onto a glass slide and subsequently sputter coated with a 10 nm SiO_2 layer to avoid any proximity interactions with the superconducting layer. Subsequently, superconducting Pb was thermally evaporated onto the SiO_2/Py film at a rate of 0.55 nm/s at room temperature in 10^{-6} Torr vacuum. The Pb film surface was dull revealing its granularity, which is common for lead films grown at room temperature. Finally, gold contacts for four-probe transport measurements were evaporated on top of the Pb film through a shadow mask.

Real-time magnetic-field penetration into these Py/SiO_2/Pb hybrid FM/SC structures was imaged magneto-optically at temperatures below the SC transition using garnet indicator films.[36] In this method, a ferrite-garnet magneto-optical indicator film is placed on top of a sample glued to the cold finger of a He-flow cryostat. Flux patterns in the sample, induced by an applied magnetic field perpen-

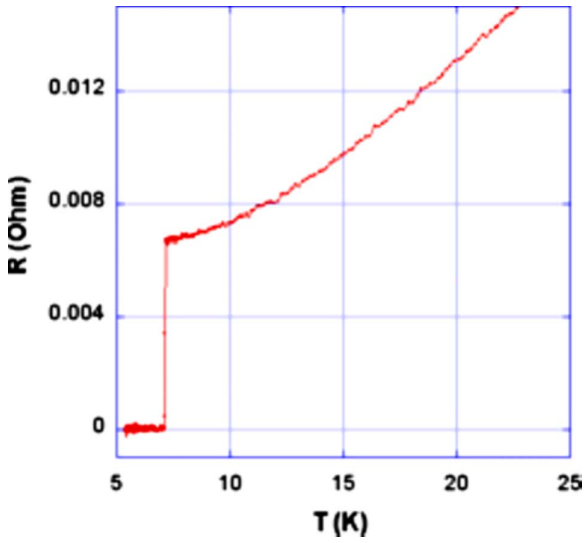

FIG. 1. (Color online) The resistive transition of lead film.

dicular to the film are imaged using a polarized light microscope. Macroscopic magnetization loops $M(H)$ below and above T_c, temperature variations in magnetization $M(T)$, resistivity curves $R(T,H)$, and voltage-current characteristics $V(I)$ at different temperatures were measured using a superconducting quantum interference device (SQUID) magnetometer and a magnetotransport setup. The domain structure in Py films was imaged at room temperature using a magnetic force microscope (MFM).

III. CHARACTERIZATION OF THE SAMPLES

Figure 1 shows the resistive transition of the Pb film in one of the samples at $T_c=7.16$ K which is close to the bulk Pb transition temperature of 7.19 K.[37,38] The transition is very narrow although the film is highly granular. Despite its large (1 μm) thickness and the superconducting type I nature of the film, it demonstrates distinct type II superconducting behavior. This is confirmed by the critical-field values obtained from the disappearance of the diamagnetic signal in the $M(T)$ curves measured on warming of the zero-field cooled sample in constant fields and from the collapse of the magnetic hysteresis loops recorded at different temperatures (Fig. 2). At $T=3$ K the diamagnetic response was observed up to fields of 2 kOe, which is much larger than the value of H_c (3 K) $\sim$ 700 Oe and the zero-temperature critical field $H_c(0)=800$ Oe of bulk and thick film Pb samples (e.g., Refs. 37 and 38, and references therein). Type II behavior of our Pb films could be expected since the film thickness is close to the critical value $d_c \sim 1$ μm for type I ($d>d_c$)/type II ($d<d_c$) crossover observed in lead films with resistance ratios of $RR=R_{300\ \mathrm{K}}/R_{T_c} \sim 50-164$.[39,40] In our films the RR value is only 21, implying a shorter coherence length and thus a stronger affinity with type II character. Estimates of the electron mean-free path (l_{eff}) from the RR and the normal-state resistivity at T_c yield $l_{\mathrm{eff}} \sim 100$ nm. This results in a coherence length of $\xi \sim 47$ nm using Pippard's formula $1/\xi = 1/\xi_0 + 1/l_{\mathrm{eff}}$ with a clean limit coherence length of lead

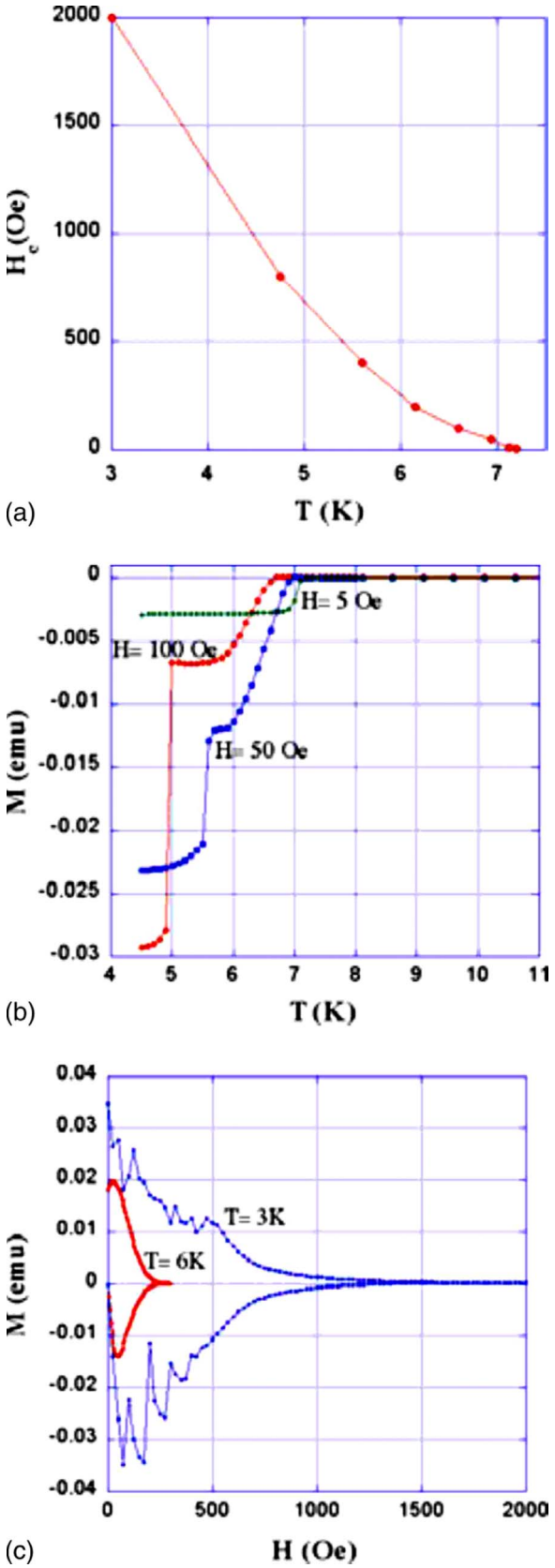

FIG. 2. (Color online) (a) Critical fields obtained from the disappearance of the diamagnetic signal on (b) $M(T)$ curves and from (c) the collapse of magnetic hysteresis loops $M(H)$ recorded at different temperatures.

$\xi_0=90$ nm.[41] We estimate the penetration depth, $\lambda=109$ nm, from the Anderson theorem[42] $\lambda\xi=\lambda_L\xi_0$ using the London penetration depth for lead $\lambda_L=57$ nm (Ref. 41) and obtain the Ginzburg-Landau parameter of $\kappa=\lambda/\xi\sim 2.3$, well within the range of type II superconductors.

The principle feature of our Py films with a standard composition of Fe81Ni19 is the growth induced *perpendicular* anisotropy K_u. Its value can be obtained from the perpendicular and in-plane magnetic saturation fields:[43] $H_\perp^{\rm sat}=4\pi M_s(1-Q)$ and $H_\parallel^{\rm sat}=2K_u/M_s$. Here, $Q=K_u/2\pi M_s^2$ is a quality factor, and M_s is the saturation magnetization. At room temperature we measure $H_\perp^{\rm sat}=10\,730$ Oe, $H_\parallel^{\rm sat}=247$ Oe, $4\pi M_s=10\,977$ G ($M_s=873$ G), yielding $K_u=1.08\times 10^5$ erg/cm^3, and $Q=0.0225$. At 8 K, $H_\perp^{\rm sat}=11\,022$ Oe, $H_\parallel^{\rm sat}=278$ Oe, $4\pi M_s=11\,300$ G ($M_s=899$ G), $K_u=1.25\times 10^5$ erg/cm^3, and $Q=0.0246$. These values are consistent with magnetic constants reported for Py of similar compositions.[44–46] The thickness of our Py film $d=0.7$ μm exceeds the critical value for the transition to the perpendicular (at $d>d_c$) magnetization state[46] $d_c=2\pi(A/K_u)^{1/2}=0.19$ μm [here the exchange constant of Py is $A=1\times 10^{-6}$ erg/cm (Ref. 45) and K_u is the room-temperature anisotropy constant] resulting in the stripe domain structure as shown in Fig. 3. Using our value of $K_u(T_{\rm room})$ to estimate the domain width[43] yields $w=(\pi d)^{1/2}[(1+Q)A/K_u]^{1/4}=0.26$ μm, in reasonable agreement with the experimental value of $w=0.44$ μm obtained from the MFM image in Fig. 3. An important feature illustrated by Fig. 3 is the possibility of aligning the stripes in any chosen direction through the application of a sufficiently strong in-plane magnetic field, as was discussed in early studies of magnetic films with perpendicular anisotropy.[47,48] Below, we show that this remarkable property can be a unique tool for manipulating the vortex motion in the adjacent SC film.

IV. RESULTS AND DISCUSSION

First we will discuss the magnetic-flux patterns in the Py/Pb hybrids observed at $T<T_c$ under increasing and decreasing magnetic fields, and then we will analyze the superconducting transport characteristics of the bilayers close to T_c. Figure 4 presents successive magneto-optical images of the magnetic-field penetration into a sample with horizontally aligned FM stripe domains. The flux enters at the sample edges, propagates inside the sample in the shape of dendrites that are highly stretched along the direction of the stripe domains, and form a nearly periodic pattern. These dendrites with an average spacing of about 35–40 μm, which is ~100 times larger than the stripe domain period, resemble thermomagnetic avalanches (TMA) (see, e.g., Ref. 49). However, in contrast to TMA they do not jump but expand continuously along the direction of stripe domains with increasing magnetic field. Their fractal appearance is due to the granularity of the Pb film, which disrupts the linear vortex motion or breaks the smooth SC current flow along the sample edges. The resulting current pattern consists of neighboring semiloops with clockwise and counterclockwise current circulations. This meandering current pattern supports opposite magnetic fields and advances the flux in those loops where the field of the screening current points in the direction of the external field [Fig. 4(b)]. The apparent periodic arrangement of the stretched dendrites seems to be the result of self-organization facilitated by film granularity and vortex guidance along the stripe domains. Under these conditions, dendritic fingers of increased vortex density initiated at the flux front cause the reduction in magnetic induction around them due to the long-range vortex repulsion.

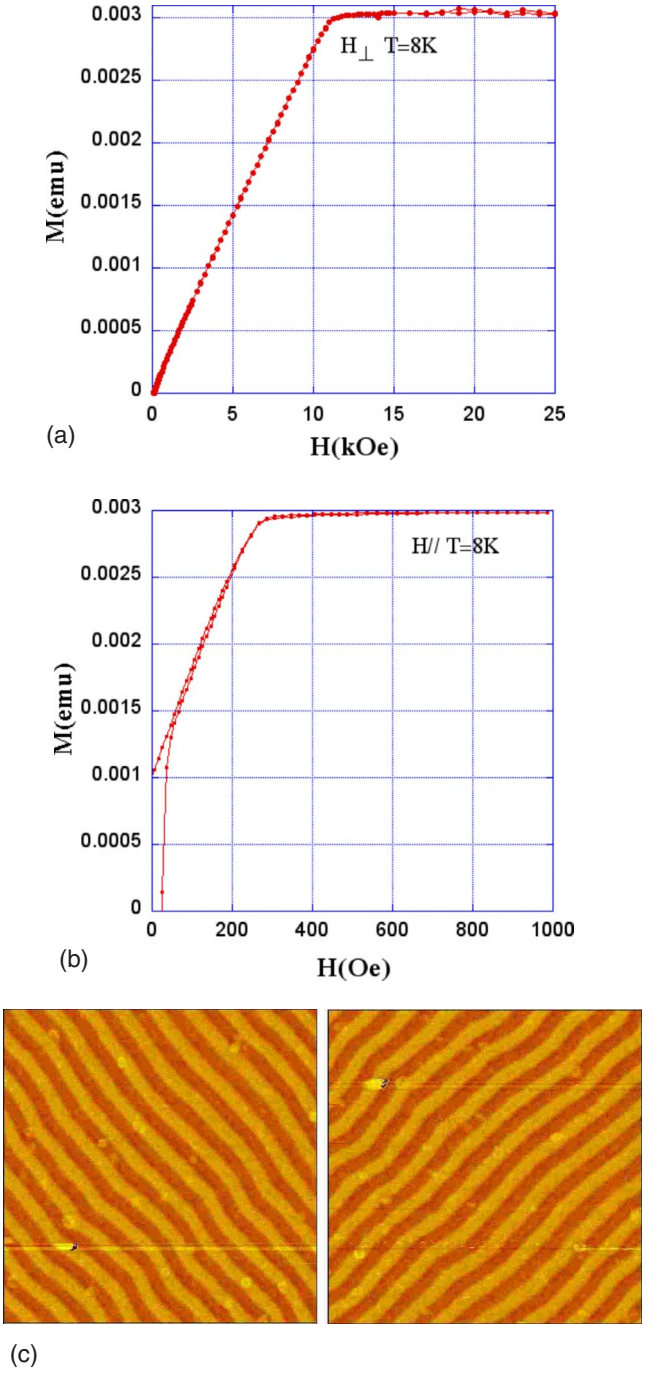

FIG. 3. (Color online) Magnetization loops of the Py film at $T=8$ K in the (a) perpendicular and (b) in-plane fields. (c) MFM pictures of the stripe domains oriented by in-plane fields in different directions.

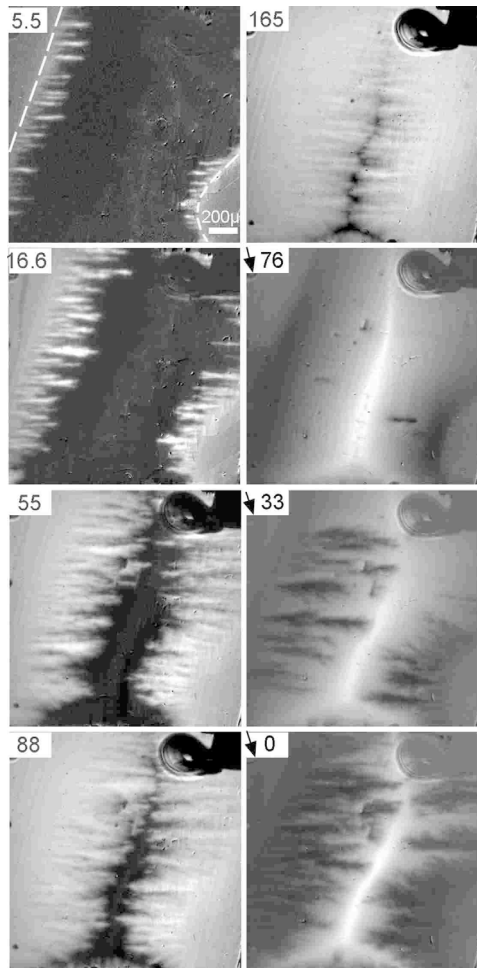

(a)

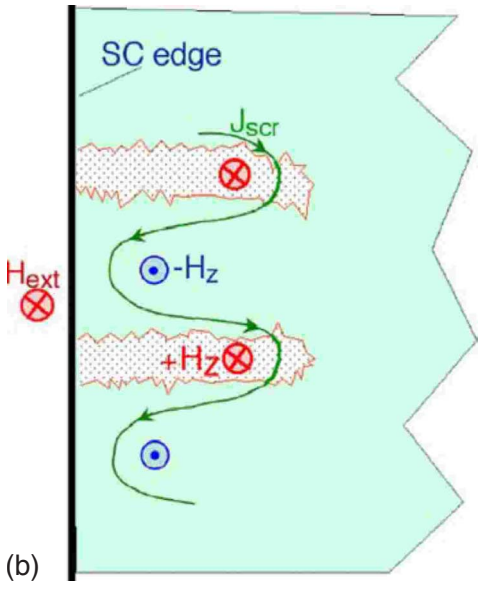

(b)

FIG. 4. (Color online) (a) Magneto-optical images of the flux penetration into the Pb/Py sample with horizontally aligned FM stripe domains at 4.2 K. Insets show fields in Oe. Pictures marked with down arrows are taken at decreasing field. (b) A scheme of meandering currents yielding spatially alternating field pattern.

Here, the *long-range* vortex interactions are controlled by the currents flowing near the top and bottom surfaces of the film, which repel the vortex ends within a surface λ layer and reduce the vortex density surrounding the flux fingers. This defines a specific periodicity that is physically similar to the periodicity of FM domains emerging from long-range magnetostatic interactions. In bulk type II superconductors, the major contribution to the intervortex forces comes from the bulk repulsion induced by their circulating supercurrents which decay exponentially at short distances $\sim\lambda$. However in films, the long-range contribution due to the algebraically decaying surface currents should not be neglected. In fact, in thin films the vortex interaction decays as the inverse of the intervortex distance.[50] Similarly, in thick samples the long-range repelling of vortex ends is expected due to their currents expanded in a λ layer near the surface.[51]

Another source of long-range vortex coupling responsible for large-scale flux periodicity could be the granularity of our lead films, which could provide a network of weak links and introduce an extended penetration depth $\lambda_J \gg \lambda$ specific to Josephson media. However, it seems the above discussed interaction of vortices through their slowly decaying surface currents is more efficient and defines the observed macroscopic periodic patterns in our samples.

Large-scale regular patterns could also appear due to the creation of thermomagnetic instabilities with a period corresponding to the k vector of the fastest growing instability mode.[52,53] However, as we mentioned above, unlike fast-jumping TMA patterns, the quasiperiodic dendrites extend slowly with increasing magnetic field, and for such slow flux diffusion, no TMA should be expected.[53]

At larger fields the average flux density increases and the flux distribution becomes more homogeneous (see Fig. 4 at 88 and 165 Oe) but the directional vortex motion is still clearly resolved. Similarly with field reduction, the flux leaves the sample preferentially along the direction of the stripe domains forming a characteristic vortex distribution complementary to the flux entry pattern (dark dendrites of reduced and inverted flux density in Fig. 4 at decreasing field of 33 and 0 Oe). A similar behavior is observed over a wide temperature range up to $T \sim 6.8$ K. At higher temperatures, the magneto-optical image contrast decreases due to the rapid decay of the critical current and it becomes difficult to obtain clear pictures of the flux distribution in the vicinity of T_c. At low temperatures ($\leq 0.6T_c$) the decrease and inversion in the field is accompanied by thermomagnetic avalanches forming large-scale dendritic patterns that are strongly branched and extent to about half of the sample width. Appropriate flux jumps are also found in the macroscopic magnetization loops delineating a remarkable jump periodicity as a function of field under certain conditions.

When the FM stripe domains are rotated by 90° with respect to the previous orientation, the flux penetration picture changes as shown in Fig. 5. Preferential flux penetration now occurs along the new orientation of the stripe domains, clearly showing that vortices are guided along the ferromagnetic domain boundaries. This picture confirms our previous conclusion that the critical current density along the domain walls is significantly larger than across them. This anisotropy results in a strong dependence of the flux penetration pattern

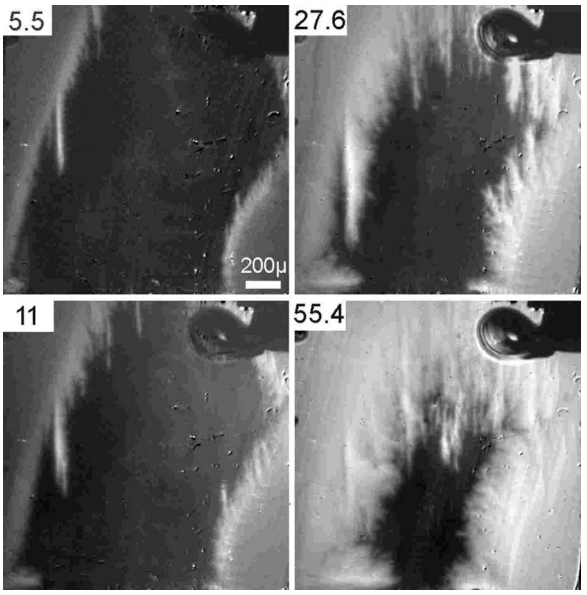

FIG. 5. MO pictures of the flux penetration when stripe domains are aligned in the vertical direction (T=4.6 K).

on the relative orientation of vortex motion and domain boundary. For instance, at the film edges that are nearly parallel to the stripe domains, flux entry is hindered and does not show any vestige of fingering. The anisotropic SC flux behavior due to the magnetic stripe domains is rather similar to the anisotropy introduced by a single direction of dense twin boundaries in $YBa_2Cu_3O_7$ crystals (Fig. 19 in Ref. 36).

In the experiments described above, the external in-plane field used to align the ferromagnetic domains was applied and then switched off at $T>T_c$ to exclude the direct effect of field on the superconductor. However, the picture does not change if the in-plane field is applied below T_c, indicating that the possible effect of in-plane vortices on the normal field penetration is much weaker and the effect of stripe domains is dominating. Once formed, the stripe magnetic domain pattern remains very stable up to reasonably high magnetic fields (~300 Oe in the film plane and ~600 Oe perpendicular to the film). It does not change with temperature cycling from 4 to ~300 K and back, and provides a very stable "imprinted" anisotropy of the superconducting currents in the hybrid.

To investigate the effect of magnetic stripe domains on the SC properties at temperatures near T_c where the magneto-optical contrast is weak, we measured current-voltage (I-V) characteristics of the samples for stripes aligned parallel and perpendicular to the current direction. Related I-V curves marked ∥ and ⊥ for T=7.11–7.17 K are shown in Fig. 6. At all temperatures the I-V curves for the parallel stripe orientation are shifted to larger currents compared to the perpendicular geometry. The difference disappears only above the superconducting transition of the Pb film. This result confirms that the domain induced anisotropy of the critical current is sustained up to T_c. The inset of Fig. 6 shows that the critical current anisotropy increases with temperature. However, the value of the anisotropy in Fig. 6 is less than what could be expected from the MO images at

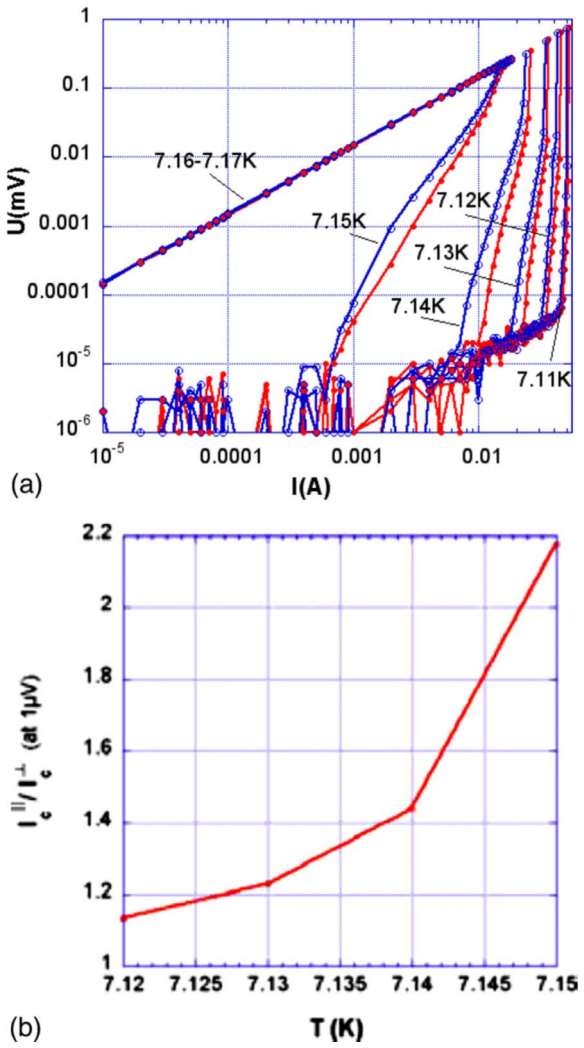

FIG. 6. (Color online) (a) I-V characteristics of the samples for stripes aligned parallel (filled circles, red) and perpendicular (open circles, blue) to the current direction. (b) The ratio of critical currents along and across the stripes close to T_c.

lower temperature. This can be due to the use of different voltage criteria in the transport measurements, where we chose J_c at 1 μV. In contrast, magneto-optical flux images reveal the final stage of slow flux motion at much smaller electric fields after a very gradual increase in the magnetic field.

At temperatures close to T_c, we found an unexpectedly large magnetoresistance in our samples. The effect was observed for currents applied perpendicular to the stripe domains in the presence of an in-plane magnetic field $H_{\text{in-pl}}$ parallel to the stripes. Figure 7 shows I-V curves obtained at T=7.11 K at various $H_{\text{in-pl}}$ values. A relatively small field of about 40 Oe can totally suppress the critical current at this temperature. At a current below the critical value for the zero-field curve, the remarkable resistance increase of more than 4 orders of magnitude can be introduced by application of only 10 Oe. The low resistance for this estimate is measured just below the critical current at the vortex creep regime, and the large resistance is measured above the critical

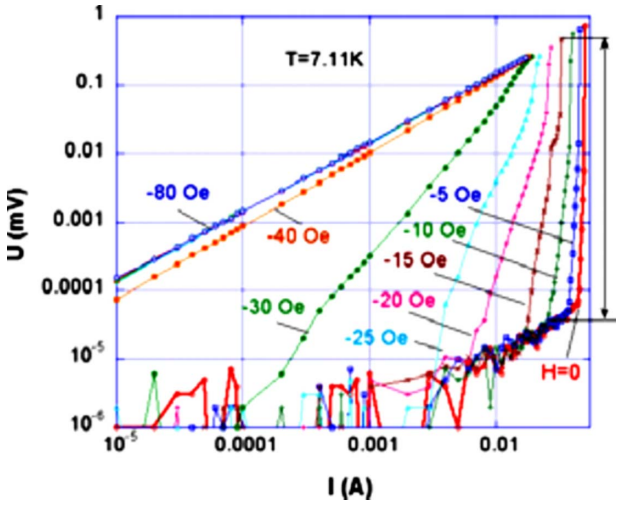

FIG. 7. (Color online) *I-V* curves at $T=7.11$ K in different $H_{\text{in-pl}}$. Arrow on the right shows the change in voltage (10 000 change of resistance) due to application of ~10 Oe along the stripes oriented perpendicular to the current direction.

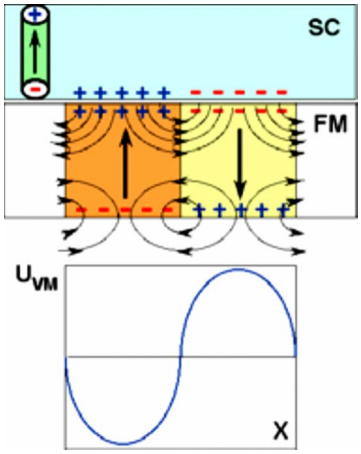

FIG. 8. (Color online) Scheme of the magnetic charges on the surface of a FM film with large perpendicular anisotropy in contact with a SC layer. In the case of the total Meissner screening, magnetic charges are doubled on the SC/FM interface compared to the free FM surface. The superconducting vortex carry magnetic charges near the SC surfaces which can be described as magnetic monopoles with a charge of two flux quanta.

current as shown by the two side arrows in Fig. 7. Such an unprecedented resistance change of $>10^6\%$ is ~1000 times larger than any magnetoresistance value reported so far (see, e.g., Refs. 33–35). This extraordinary magnetoresistance could be the result of granularity of our Pb film, producing a network of weak links that are suppressed by small in-plane fields near T_c and facilitate easier flux flow along the domains. The resulting dissipation due to fast moving vortices and consequent heating breaks the superconducting state and switches the sample to the normal resistance regime.

V. EFFECTS OF THE MAGNETIC DOMAIN STRUCTURE ON SUPERCONDUCTING PARAMETERS

The idea of using ferromagnetic domains for manipulating superconducting properties has long been discussed theoretically,[20,25,54–60] and recently it was a subject of extensive experimental research.[14,61–65] The experimental results were mostly related to the detrimental effect of the FM domain stray fields on the SC order parameter[17,66] or to the enhanced dissipation due to the stray field induced vortex flow.[67] In some cases, however, superconductivity could be locally enhanced by external fields H_{ex} compensating the stray field in domains magnetized against H_{ex}.[68] Also, stronger superconductivity was expected along the "field-free" domain walls.[14,16,69]

Following earlier reports,[14,15] it was tempting to assign the preferential SC current flow along the stripes to domain-wall superconductivity, which originates from a stronger suppression of the SC order parameter by the stray fields in the domains rather than at their boundaries. However, a thorough analysis of the stray fields shows that their values at the domain boundaries is practically the same as in the center of the domains and only their orientation turns along the film plane. In this case only SC layers of thickness d that are much smaller than the coherence length ξ could have in-plane critical fields $H_{c\|} \sim 2\sqrt{6} H_c \lambda / d$ [Ref. 70, p. 131] that are much larger than the perpendicular critical field $H_{c\perp} = H_{c2} \sim H_c \lambda \sqrt{2}/\xi$ (here H_c and λ are the bulk critical field and the penetration depth), and thus could cause weaker suppression of superconductivity (higher T_c) along the domain walls. Our lead films are much thicker than ξ and the above mechanism of the domain-wall superconductivity is not applicable.

The observed highly directed penetration of vortices along the stripe domains and the resulting strong anisotropy of the critical current can be explained by the enhanced pinning of vortices at the magnetic domain walls hindering the propagation of vortices across the stripes. Bulaevskii *et al.*[25] were the first to emphasize the high efficiency of the domain-wall pinning in SC/FM bilayers with stripe domain structures. Later, the effect was discussed in several theoretical works[56–59,71,72] and explored experimentally in hybrids with different parameters of the SC and FM components. In some works, only the suppression of superconductivity due to the stray fields of the FM domains was reported.[65,66,73] Meanwhile, the majority of experiments on various combinations of FM substrates and low-T_c and high-T_c SC films found increased pinning in the multidomain states of FMs.[62,74,75] The maximum pinning enhancement in Refs. 62, 74, and 75 was observed for isolated bubble or dendritic domains formed near the FM saturation. However, the pinning effect of domain boundaries was not directly demonstrated until our recent work, where the vortex guidance along the stripe domains was imaged in a $NbSe_2$ crystal covered with a Py film.[32]

Our observations of vortex motion in Pb/Py bilayers are qualitatively similar to the flux behavior in a $NbSe_2$ crystal coated with Py.[32] They can be understood within a picture of vortex coupling to the magnetization in magnetic domains in relatively thick FM and SC layers.[72] This coupling is schematically illustrated in Fig. 8 where pluses and minuses show the distribution of the fictitious magnetic charges creating the magnetic fields. At the same time, the magnetic

field of the vortices can be described as fields of magnetic monopoles with charges of two flux quanta $2\Phi_0$.[51] Using the field distributions for stripe domains in a high anisotropy FM film, the coupling energy can be written as[72]

$$U_{\mathrm{VM}} = \pm (2\Phi_0 M_s/\pi) \int_0^{x_i} \ln[\tan(\pi x/2d)]dx. \qquad (1)$$

Here + and − correspond to the domains polarized against and along the vortex flux direction, respectively, and x_i is a position of vortex with respect to the nearest domain wall. Note that the derivative of the integral in Eq. (1), yielding the pinning force, represents the *in-plane* stray field on the FM surface, $H_x(0)$, due to domains homogeneously magnetized up and down perpendicular to the film. This field is maximum at the domain wall. The model should be modified for Py, which has moderate anisotropy so that the domains are not homogeneously magnetized perpendicular to the surface but form a twisted structure (detailed micromagnetic simulations can be found, e.g., in Refs. 45 and 46). Here, magnetic charges ($\rho_m = -4\pi$ div **M**, where **M** is the FM magnetization vector) form not only at the surface but are also distributed in the volume. The resulting stray fields are weaker than in high-Q materials and possess a smoother profile. Assuming a sinusoidal surface magnetic potential and a stray field distribution with amplitude derived from numerical simulations of $H_x(0) \sim 0.3M_s$,[45] we can estimate the pinning force due to the interaction of the vortex charge and the FM stray fields[72] as $F_p \sim 0.3\Phi_0 M_s/4\pi$. Here we neglected the doubling of the magnetic charge at the FM/SC interface assuming that the stray fields of the domains are not screened but rather frozen into the SC as the sample is cooled below T_c. For straight vortices in a $d=1$ μm-thick film, this would correspond to $J_c^{\mathrm{DW}} = F_p \times 10/(d\Phi_0)[\mathrm{A/cm^2}] \sim 2.15 \times 10^6$ A/cm^2. This estimate is much larger than the experimental value of $J_c(H=0) \sim 0.25 \times 10^4$ A/cm^2 measured at 7.11 K. One reason could be that, near the surface of the Py film, the transitions between up and down magnetized domains are very wide and should produce smaller $H_x(0)$ compared to the field of a zero width domain wall in the model[72] which yields nearly diverging in-plane fields at the domain boundary. Another reason could be the formation of a network of weak links with large penetration depth ($\lambda_J \gg \lambda$) due to the granularity of our Pb film. In both cases the energy scale of the vortex-domain interactions will be defined by $\sim\Phi_0 H_x$ although their characteristic length scale (l) will be much larger than λ and thus lead to much smaller pinning force ($F_p \sim U_{\mathrm{VM}}/l$).

VI. GIANT MAGNETORESISTANCE

A remarkable effect observed in our samples is the extremely large magnetoresistance of $\sim 10^6$% measured at $T \sim T_c$ in small in-plane fields of ~ 10 Oe. Earlier experiments on FM/SC hybrids reported ~ 3 orders of magnitude smaller values.[33–35] The effect was measured for stripes oriented perpendicular to the current direction and the field applied along the stripes. The direct field suppression of superconductivity in our films should not be significant because perpendicular critical fields [Fig. 2(a)] are noticeably larger than those yielding a strong resistivity change and there is no reason for smaller parallel H_{c2}. It could be expected that the in-plane fields tilt the magnetization of the Py stripe domains toward the film plane, and thus reduce the normal stray fields and enhance the superconductivity. Instead, we observe a strong suppression of the SC currents. This could again originate from the electromagnetic properties of the weak-link network in our granular Pb films, which becomes more effective at higher temperatures. The observed enhanced magnetoresistance can be due to the suppression of weak links by the in-plane magnetic field. This could initiate both the motion along the stripes of current generated vortices perpendicular to the film, and motion from the top to the bottom surface of the film of field induced vortices that are parallel to the film. The rapid vortex flow induces heat generation which progressively transforms the superconducting sample into the normal state resulting in the sharp I-V curve observed in the experiment. Naturally, at larger critical currents (smaller applied fields) the vortex motion and the resulting heat dissipation should be faster and cause even sharper transitions to the normal state in accordance with data shown in Fig. 7. In this case, the progressive heat generation could result in a thermal runaway that would produce a stepwise transition to the normal state. However, in some of our measured I-V characteristics, we recorded several intermediate points in the sharp rising section of the I-V curves which contradict the thermal runaway scenario. A better understanding of the effect will be reached only after more detailed investigations.

VII. CONCLUSIONS

We imaged magneto-optically and confirmed by transport measurements a preferential motion of vortices along stripe domains in Py/Pb FM/SC hybrid films. In the SC films the effect is much more pronounced than observed recently in $NbSe_2$ crystals covered with Py.[32] Alignment of FM stripe domains in Py along any chosen direction in the film plane forms a robust anisotropy of the flux propagation and current flow in the SC Pb film. Due to the Pb film granularity vortices self-organize in a quasiperiodic pattern with dendritic fingers of a high-flux density separated by low induction regions and stretched along the direction of stripes. We suggest that the macroscopic regularity of the pattern is defined by the magnetic fields emanating from the flux fingers, which repel vortices in the neighboring regions acting on their ends near the surface. This is qualitatively similar to the formation of periodic domains due to magnetic stray fields in ferromagnets.

Transport measurements at larger temperatures, when the MO contrast is too weak for imaging, confirm the enhanced motion of vortices along the stripe domains showing smaller critical currents across the stripes (larger J_c along the stripes). The effect is observed up to temperatures very close to T_c and the anisotropy of critical currents grows with increasing temperature.

The extremely large magnetoresistance of $\sim 10^6$% is found for currents perpendicular to the stripe domains in small in-plane fields along the stripes. The high field sensitivity of the transport properties at temperatures close to T_c

could be associated with the granular structure of the film. Suppression of the weak links by the in-plane field and the resulting speeding up of current induced vortices moving along the stripes, and field induced vortices moving from top to the bottom of the Pb film may cause the progressive heat generation, forming sharp *I-V* curves susceptible to the small field changes.

The studied effect shows a possibility of the soft magnetic lithography allowing the creation of the tunable pinning potential in a SC component of the hybrid. It can allow the design of cryogenic devices based on the FM/SC hybrids, e.g., a robust current switch with the memory effect manipulated by the rotation of stripe domains.

ACKNOWLEDGMENTS

The authors are grateful to E. B. Sonin and N. B. Kopnin for useful discussions. The submitted paper was created by the University of Chicago, Argonne, LLC, Operator of Argonne National Laboratory "Argonne." Argonne, a U.S. Department of Energy, Office of Science Laboratory, is operated under Contract No. DEAC02-06CH11357.

*Present address: MSD and Center for Nanoscale Materials, Argonne National Laboratory, Argonne, Illinois 60439, USA.

[1] V. A. Vas'ko, V. A. Larkin, P. A. Kraus, K. R. Nikolaev, D. E. Grupp, C. A. Nordman, and A. M. Goldman, Phys. Rev. Lett. **78**, 1134 (1997).
[2] C.-C. Fu, Z. Huang, and N.-C. Yeh, Phys. Rev. B **65**, 224516 (2002).
[3] Z. Sefrioui, M. Varela, V. Peña, D. Arias, C. León, J. Santamaría, J. E. Villegas, J. L. Martínez, W. Saldarriaga, and P. Prieto, Appl. Phys. Lett. **81**, 4568 (2002).
[4] F. Chen, B. Gorshunov, G. Cristiani, H.-U. Habermeier, and M. Dressel, Solid State Commun. **131**, 295 (2004).
[5] L. Fratila, I. Maurin, C. Dubourdieu, and J. C. Villégier, Appl. Phys. Lett. **86**, 122505 (2005).
[6] H. Yamazaki, N. Shannon, and H. Takagi, Phys. Rev. B **73**, 094507 (2006).
[7] A. I. Buzdin and V. V. Ryazanov, C. R. Phys. **7**, 107 (2006).
[8] A. I. Buzdin, A. V. Vedyayev, and N. Ryzhanova, Europhys. Lett. **48**, 686 (1999).
[9] L. R. Tagirov, Phys. Rev. Lett. **83**, 2058 (1999).
[10] J. Y. Gu, C. Y. You, J. S. Jiang, J. Pearson, Y. B. Bazaliy, and S. D. Bader, Phys. Rev. Lett. **89**, 267001 (2002).
[11] I. Baladie and A. Buzdin, Phys. Rev. B **67**, 014523 (2003).
[12] A. I. Buzdin and A. S. Mel'nikov, Phys. Rev. B **67**, 020503(R) (2003).
[13] A. Y. Aladyshkin, A. I. Buzdin, A. A. Fraerman, A. S. Mel'nikov, D. A. Ryzhov, and A. V. Sokolov, Phys. Rev. B **68**, 184508 (2003).
[14] Z. R. Yang, M. Lange, A. Volodin, R. Szymczak, and V. V. Moshchalkov, Nature Mater. **3**, 793 (2004).
[15] W. Gillijns, A. Y. Aladyshkin, M. Lange, M. J. Van Bael, and V. V. Moshchalkov, Phys. Rev. Lett. **95**, 227003 (2005).
[16] A. Y. Aladyshkin and V. V. Moshchalkov, Phys. Rev. B **74**, 064503 (2006).
[17] W. Gillijns, A. Y. Aladyshkin, A. V. Silhanek, and V. V. Moshchalkov, Phys. Rev. B **76**, 060503(R) (2007).
[18] Y. A. Izyumov, Y. N. Proshin, and M. G. Khusainov, Phys. Usp. **45**, 109 (2002).
[19] A. I. Buzdin, Rev. Mod. Phys. **77**, 935 (2005).
[20] I. F. Lyuksyutov and V. L. Pokrovsky, Adv. Phys. **54**, 67 (2005).
[21] F. S. Bergeret, A. F. Volkov, and K. B. Efetov, Appl. Phys. A: Mater. Sci. Process. **89**, 599 (2007).
[22] J. I. Martin, M. Velez, J. Nogues, and I. K. Schuller, Phys. Rev. Lett. **79**, 1929 (1997).
[23] Y. Jaccard, J. I. Martin, M. C. Cyrille, M. Velez, J. L. Vicent, and I. K. Schuller, Phys. Rev. B **58**, 8232 (1998).
[24] J. I. Martin, M. Velez, A. Hoffmann, I. K. Schuller, and J. L. Vicent, Phys. Rev. Lett. **83**, 1022 (1999).
[25] L. N. Bulaevskii, E. M. Chudnovsky, and M. P. Maley, Appl. Phys. Lett. **76**, 2594 (2000); L. N. Bulaevskii, E. M. Chudnovsky, and M. Daumens, Phys. Rev. B **66**, 136502 (2002).
[26] M. J. Van Bael, J. Bekaert, K. Temst, L. Van Look, V. V. Moshchalkov, Y. Bruynseraede, G. D. Howells, A. N. Grigorenko, S. J. Bending, and G. Borghs, Phys. Rev. Lett. **86**, 155 (2001).
[27] M. J. Van Bael, L. Van Look, M. Lange, K. Temst, G. Guntherodt, V. V. Moshchalkov, and Y. Bruynseraede, J. Supercond. **14**, 355 (2001).
[28] M. Lange, M. J. Van Bael, and V. V. Moshchalkov, J. Low Temp. Phys. **139**, 195 (2005).
[29] J. E. Villegas, K. D. Smith, L. Huang, Y. M. Zhu, R. Morales, and I. K. Schuller, Phys. Rev. B **77**, 134510 (2008).
[30] J. E. Villegas, C.-P. Li, and I. K. Schuller, Phys. Rev. Lett. **99**, 227001 (2007).
[31] A. Hoffmann, L. Fumagalli, N. Jahedi, J. C. Sautner, J. E. Pearson, G. Mihajlovic, and V. Metlushko, Phys. Rev. B **77**, 060506(R) (2008).
[32] V. Vlasko-Vlasov, U. Welp, G. Karapetrov, V. Novosad, D. Rosenmann, M. Iavarone, A. Belkin, and W.-K. Kwok, Phys. Rev. B **77**, 134518 (2008).
[33] V. Pena, Z. Sefrioui, D. Arias, C. Leon, J. Santamaria, J. L. Martinez, S. G. E. te Velthuis, and A. Hoffmann, Phys. Rev. Lett. **94**, 057002 (2005).
[34] G. X. Miao, K. S. Yoon, T. S. Santos, and J. S. Moodera, Phys. Rev. Lett. **98**, 267001 (2007).
[35] D. Stamopoulos, E. Manios, and M. Pissas, Phys. Rev. B **75**, 184504 (2007).
[36] V. K. Vlasko-Vlasov, U. Welp, G. W. Crabtree, and V. I. Nikitenko, in *Physics and Materials Science of Vortex States, Flux Pinning and Dynamics*, NATO Advanced Studies Institute, Series E: Applied Science Vol. 356, edited by R. Kossowsky, S. Bose, V. Pan, and Z. Durusoy (Kluwer, London, 1999), p. 205.
[37] G. Chanin and J. P. Torre, Phys. Rev. B **5**, 4357 (1972).
[38] N. Suresh and J. L. Tallon, Phys. Rev. B **75**, 174502 (2007).
[39] G. D. Cody and R. E. Miller, Phys. Rev. **173**, 481 (1968).
[40] G. L. Dolan, J. Low Temp. Phys. **15**, 133 (1974).
[41] A. Suter, E. Morenzoni, R. Khasanov, H. Luetkens, T. Prokscha, and N. Garifianov, Phys. Rev. Lett. **92**, 087001 (2004).
[42] P. W. Anderson, J. Phys. Chem. Solids **11**, 26 (1959).

[43] Y. Murayama, J. Phys. Soc. Jpn. **21**, 2253 (1966).
[44] Y. Sugita, H. Fujivara, and T. Saito, Appl. Phys. Lett. **10**, 229 (1967).
[45] B. B. Pant and K. Matsuyama, Jpn. J. Appl. Phys., Part 1 **32**, 3817 (1993).
[46] J. Ben Youssef, N. Vukadinovic, D. Billet, and M. Labrune, Phys. Rev. B **69**, 174402 (2004).
[47] N. Saito, H. Fujivara, and Y. Sugita, J. Phys. Soc. Jpn. **19**, 1116 (1964).
[48] A. J. Kurtzig and F. B. Hagedorn, IEEE Trans. Magn. **7**, 473 (1971).
[49] R. J. Wijngaarden, M. S. Welling, C. M. Aegerter, and M. Menghini, Eur. Phys. J. B **50**, 117 (2006).
[50] L. Pearl, Appl. Phys. Lett. **5**, 65 (1964).
[51] G. Carneiro and E. H. Brandt, Phys. Rev. B **61**, 6370 (2000).
[52] A. L. Rakhmanov, D. V. Shantsev, Y. M. Galperin, and T. H. Johansen, Phys. Rev. B **70**, 224502 (2004).
[53] I. S. Aranson, A. Gurevich, M. S. Welling, R. J. Wijngaarden, V. K. Vlasko-Vlasov, V. M. Vinokur, and U. Welp, Phys. Rev. Lett. **94**, 037002 (2005).
[54] E. B. Sonin, Pis'ma Zh. Tekh. Fiz. **14**, 1640 (1988) [Sov. Tech. Phys. Lett. **14**, 714 (1988)].
[55] Y. I. Bespyatykh and W. Wasilevski, Phys. Solid State **43**, 224 (2001).
[56] Y. I. Bespyatykh, W. Wasilevski, M. Gajdek, I. P. Nikitin, and S. A. Nikitov, Phys. Solid State **43**, 1827 (2001).
[57] Y. I. Bespyatykh, V. Vasilevskii, V. I. Voronov, and S. A. Nikitov, J. Commun. Technol. Electron. **48**, 207 (2003).
[58] S. Erdin, I. F. Lyuksyutov, V. L. Pokrovsky, and V. M. Vinokur, Phys. Rev. Lett. **88**, 017001 (2001).
[59] M. A. Kayali and V. L. Pokrovsky, Phys. Rev. B **69**, 132501 (2004).
[60] S. Erdin, Phys. Rev. B **73**, 224506 (2006).
[61] A. Garcıa-Santiago, F. Sanchez, M. Varela, and J. Tejada, Appl. Phys. Lett. **77**, 2900 (2000).
[62] M. Lange, M. J. Van Bael, V. V. Moshchalkov, and Y. Bruynseraede, Appl. Phys. Lett. **81**, 322 (2002).
[63] A. Yu. Rusanov, M. Hesselberth, J. Aarts, and A. I. Buzdin, Phys. Rev. Lett. **93**, 057002 (2004).
[64] F. Laviano, L. Gozzelino, E. Mezzetti, P. Przyslupski, A. Tsarev, and A. Wisniewski, Appl. Phys. Lett. **86**, 152501 (2005).
[65] D. Stamopoulos, Supercond. Sci. Technol. **19**, 652 (2006); D. Stamopoulos and M. Pissas, Phys. Rev. B **73**, 132502 (2006).
[66] A. Singh, C. Suergers, M. Uhlarz, S. Singh, and H. Von Lohneysen, Appl. Phys. A: Mater. Sci. Process. **89**, 593 (2007).
[67] C. Bell, S. Tursucu, and J. Aarts, Phys. Rev. B **74**, 214520 (2006).
[68] Z. R. Yang, J. Van de Vondel, W. Gillijns, W. Vinckx, V. V. Moshchalkov, and R. Szymczak, Appl. Phys. Lett. **88**, 232505 (2006).
[69] A. Y. Rusanov, T. E. Golikova, and S. V. Egorov, JETP Lett. **87**, 175 (2008).
[70] M. Tinkham, *Introduction to Superconductivity* (McGraw-Hill, New York, 1996).
[71] E. B. Sonin, Phys. Rev. B **66**, 136501 (2002).
[72] R. Laiho, E. Lahderanta, E. B. Sonin, and K. B. Traito, Phys. Rev. B **67**, 144522 (2003).
[73] T. Hu, H. Xao, C. Visani, Z. Sefrioui, J. Santamaria, and C. C. Almasan, Physica B **403**, 1167 (2008).
[74] D. B. Jan, J. Y. Coulter, M. E. Hawley, L. N. Bulaevskii, M. P. Maley, Q. X. Jia, B. B. Maranville, F. Hellman, and X. Q. Pan, Appl. Phys. Lett. **82**, 778 (2003).
[75] M. Z. Cieplak, X. M. Cheng, C. L. Chien, and H. Sang, J. Appl. Phys. **97**, 026105 (2005).